

SELECTIVE RETINAL THERAPY WITH MICROSECOND EXPOSURES USING A CONTINUOUS LINE SCANNING LASER

YANNIS M. PAULUS, MD,* ATUL JAIN, MD,* HIROYUKI NOMOTO, MD, PhD,*
CHRISTOPHER SRAMEK, PhD,† RAY F. GARIANO, MD, PhD,* DAN ANDERSEN, BS,‡
GEORG SCHUELE, PhD,‡ LOH-SHAN LEUNG, MD, MS,* THEODORE LENG, MD,*
DANIEL PALANKER, PhD*†

Purpose: To evaluate the safety, selectivity, and healing of retinal lesions created using a continuous line scanning laser.

Methods: A 532-nm Nd:YAG laser (PASCAL) with retinal beam diameters of 40 μm and 66 μm was applied to 60 eyes of 30 Dutch-belted rabbits. Retinal exposure duration varied from 15 μs to 60 μs . Lesions were acutely assessed by ophthalmoscopy and fluorescein angiography. Retinal pigment epithelial (RPE) flatmounts were evaluated with live–dead fluorescent assay. Histological analysis was performed at 7 time points from 1 hour to 2 months.

Results: The ratios of the threshold of rupture and of ophthalmoscopic visibility to fluorescein angiography visibility (measures of safety and selectivity) increased with decreasing duration and beam diameter. Fluorescein angiography and live–dead fluorescent assay yielded similar thresholds of RPE damage. Above the ophthalmoscopic visibility threshold, histology showed focal RPE damage and photoreceptor loss at 1 day, without inner retinal effects. By 1 week, photoreceptor and RPE continuity was restored. By 1 month, photoreceptors appeared normal.

Conclusion: Retinal therapy with a fast scanning continuous laser achieves selective targeting of the RPE and, at higher power, of the photoreceptors without permanent scarring or inner retinal damage. Continuous scanning laser can treat large retinal areas within standard eye fixation time.

RETINA X:1–9, 2010

Since its introduction nearly 40 years ago, laser photocoagulation remains the standard of care for many retinopathies.^{1,2} By destroying retinal cells, panretinal laser photocoagulation is assumed to reduce

metabolic demand to match the poor perfusion of ischemic retina. Production of hypoxia-inducible angiogenic factors is thereby reduced and retinal neovascularization regresses.^{3–6} Because photoreceptors are the most numerous and metabolically active cells in the retina (containing large numbers of mitochondria), the therapeutic effect of panretinal laser photocoagulation in ischemic diseases, such as proliferative diabetic retinopathy, is likely achieved by the destruction of a fraction of the photoreceptors, without needing to damage the inner retina.

In conventional retinal photocoagulation, pulse durations are typically from 100 milliseconds to 200 milliseconds, laser spot diameters are from 100 μm to 500 μm , and powers range from 100 mW to 750 mW.^{7–9} These parameters produce ophthalmoscopically visible gray–white lesions because of the thermal denaturation (coagulation) of photoreceptors and the inner retina. Heat is produced by light

From the *Department of Ophthalmology, Stanford University School of Medicine, Stanford, California; †Hansen Experimental Physics Laboratory, Stanford, California; and ‡OptiMedica Inc, Santa Clara, California.

Funding was provided in part by the Alcon Research Institute, the Horgren and Miller Family Foundations, OptiMedica, Corp, Air Force Office of Scientific Research, the Heed Ophthalmic Foundation, and the Angelos and Penelope Dellaporta Research Fund.

D. Andersen and G. Schuele are employees of OptiMedica Corporation.

D. Palanker holds a Stanford University patent on patterned scanning laser photocoagulation licensed to OptiMedica Corporation with an associated equity and royalty interest and serves as a consultant for OptiMedica Corporation.

Reprint requests: Yannis Paulus, MD, Eye Institute at Stanford, 2452 Watson Court, Palo Alto, CA 94303-5353; e-mail: ypaulus@stanford.edu

absorption in pigmented cells, predominantly in the retinal pigment epithelium (RPE) and choroid, and subsequently diffuses into the inner retina.^{10–12}

However, conventional photocoagulation application has significant side effects such as pain during treatment; permanent retinal scarring; and decreased peripheral, color, and night visions.^{13–16} Retinal scars can initiate infiltrative/inflammatory processes involving additional cell loss; can enlarge postoperatively;^{17–19} and can cause choroidal neovascularization,^{20,21} subretinal fibrosis,^{22–24} and additional visual field loss.^{25–29}

Recent evidence has shown that photocoagulation lesion size decreases over time in rodents³⁰ and rabbits.¹⁵ This effect is especially profound in smaller and less intense laser lesions, where a significant decrease of the initial damage zone in the photoreceptor layer has been demonstrated, suggesting shifting of the photoreceptors from unaffected areas to the initially acellular lesion center.¹⁵ A similar phenomenon has been observed in snake eyes.³¹

A new method of retinal photocoagulation termed pattern scanning laser photocoagulation (PASCAL) allows for patterns of 4 to 56 burns to be applied in <1 second using a scanning laser with shorter pulse durations (10–30 milliseconds).³² Retinal lesions produced by this system are more confined to the RPE and photoreceptor layers.¹⁴ In addition, because of reduced heat diffusion into the choroid, shorter pulse duration treatment was found to be less painful than conventional laser.^{33–35}

Many diseases involving the macula, such as age-related macular degeneration, diabetic macular edema, and central serous chorioretinopathy (CSC), are thought to involve dysfunction of the RPE. This suggests that RPE-specific treatments might help in these conditions, while avoiding destruction of photoreceptors. The first RPE-selective retinal laser treatment was achieved using 5-microsecond argon laser pulses at 514 nm and a repetition rate of 500 Hz in rabbit eyes.³⁶ It has been shown that microsecond pulses can produce intracellular microbubbles around melanosomes, leading to selective death of RPE cells while the surrounding retinal temperature remains sublethal.³⁷ Selective RPE treatment without photoreceptor damage was termed “selective retinal therapy” (SRT). Preliminary clinical trials conducted with an Nd:YLF laser using pulse durations of 1.7 microseconds have demonstrated no visual loss after the treatment, as confirmed by microperimetry.³⁸ Spectral-domain optical coherence tomography imaging in humans has demonstrated unaffected neural retina and RPE thinning at 1 hour and normal neural retina and RPE at 1 year after SRT.³⁹ At energies

corresponding to selective damage of the RPE, SRT does not produce an immediate ophthalmoscopically visible retinal lesion.⁴⁰

In 2000, the first clinical study reported the efficacy of SRT in 12 patients with diabetic maculopathy, 10 patients with soft drusen, and 4 with CSC.³⁸ Selective retinal therapy has shown promise in other small clinical trials for treating CSC⁴¹ and diabetic macular edema.⁴² Selective retinal therapy is currently being investigated for its utility in treating drusen and branch retinal vein occlusion. Preliminary results from an international multicenter trial have been reported to be quite promising among 60 patients with diabetic maculopathy and 10 patients with CSC.⁴³ However, SRT requires a dedicated clinical system that entails additional cost, and such systems have not yet gained widespread acceptance in clinical practice.^{44–46}

Microsecond exposures can also be produced with a continuous scanning laser. With appropriately high scanning speed, selective RPE damage has been recently demonstrated.⁴⁷ However, that system used a narrow beam of 18 μm , which is unlikely to become practical for clinical application because of the difficulty of very tight focusing with a slit-lamp-based optical system.

This study evaluates the possibility of using a clinically available scanning laser system for selective RPE treatment in a continuous line scanning mode. We assess the safety and selectivity of the treatment at various scanning velocities and beam sizes and also measure the thresholds of ophthalmoscopic and angiographic visibility, RPE cellular viability, and rupture of Bruch’s membrane. We also histologically examine the dynamics and extent of healing of the retinal lesions from 1 hour to 2 months.

Materials and Methods

Scanning Laser System With Microsecond Dwell Time

A 532-nm Nd:YAG laser (PASCAL; OptiMedica, Inc, Santa Clara, CA) provided optical radiation coupled into a multimode step index optical fiber. The exit surface of the fiber is telecentrically imaged through the scanning system onto the retina, providing a variety of spot sizes with top-hat intensity profiles. At the aerial image plane of the slit-lamp microscope, the laser spots measured 400 μm , 200 μm , 100 μm , and 60 μm in diameter, with the laser intensity transition from 10% to 90% occurring over 6 μm . Variation of the beam intensity within the flat-top area did not exceed $\pm 7\%$. The software controlling the system was modified for rapid scanning of the laser to achieve

microsecond dwell times, with a scanning speed up to 6.6 m/s, limited by the galvanometric mirror actuators.

The graphical user interface was used to control laser parameters, including the beam diameter, laser power, scanning velocity, aiming beam intensity, line length, number of lines (1–3) in the pattern, spacing between the lines, and pattern repetition rate. Once the treatment parameters were appropriately selected, a foot pedal was used to activate the laser.

Retinal exposure duration, or beam dwell time, is defined as the beam diameter divided by the scanning velocity and corresponds to the maximum amount of time the RPE cells are exposed to the laser light. For example, for an aerial beam diameter of 100 μm and a velocity of 6.6 m/s, the exposure duration would be 15 microseconds.

Retinal Laser Application

Thirty Dutch-belted rabbits (weight, 1.5–2.5 kg) were used in accordance with the Association for Research in Vision and Ophthalmology Statement Regarding the Use of Animals in Ophthalmic and Vision Research, after approval from the Stanford University Animal Institutional Review Board. The rabbits were anesthetized using ketamine hydrochloride (35 mg/kg, intramuscularly), xylazine (5 mg/kg, intramuscularly), and glycopyrrolate (0.01 mg/kg, intramuscularly) administered 15 minutes before the procedure. Pupillary dilation was achieved by 1 drop each of 1% tropicamide and 2.5% phenylephrine hydrochloride. One drop of topical tetracaine 0.5% was instilled in each eye before treatment.

A Mainster standard retinal laser contact lens (model no. OMRA-S; Ocular Instruments, Bellevue, WA) was used to focus the laser on the rabbit fundus. Taking into account the combined magnifications of the contact lens and rabbit eye ($\times 0.66$),⁴⁸ the aerial image of 100 μm and 60 μm corresponded to retinal spot size of 66 μm and 40 μm , respectively. Using the line scanning software, line patterns were applied in either single or triple lines separated by two line diameters. Conventional, intense marker spot lesions were placed adjacent to the lines to facilitate later histological localization of the barely visible and invisible line lesions.

Retinal Histology

Rabbits were killed at 1 hour, 1 and 3 days, 1 and 2 weeks, and 1 and 2 months after treatment with a lethal dose of Beuthanasia (150 mg/kg, intravenously) injected into the marginal ear vein or, in cases in which intravenous injection was unable to be achieved, injected intracardially. Eyes were enucleated and fixed

in 1.25% glutaraldehyde/1% paraformaldehyde in cacodylate buffer at pH 7.2 overnight at room temperature. The eyes were then postfixed in osmium tetroxide, dehydrated with a graded series of ethanol, processed with propylene oxide, embedded in an epoxy resin, and sectioned into 1- μm -thick sections. Samples were stained with toluidine blue and examined by light microscopy.⁴⁹

Serial sections of the retina were examined, and 12 lines from 2 different animals (4 eyes) were analyzed for each of the 7 time points and scanning laser parameter settings. Lesion width was measured as the furthest extent of damage visible along the RPE–photoreceptor junction. The mean and standard deviation of these numbers were calculated using Microsoft Excel.

Measurement of Visibility and Rupture Thresholds

The clinical appearance of the laser lesions (ophthalmoscopic visibility and rupture) were graded by a single masked observer 30 seconds after the treatment. A rupture of Bruch's membrane was assumed to occur if small bubbles with or without hemorrhage appeared at the lesion site. The visibility limit was described as any faint lightening of the fundus pigmentation that corresponded with the area of laser application. The 30-second delay was selected because it represents a reasonable estimate for how long ophthalmologists might look at any given area of retina during the treatment. The longer follow-up with ophthalmoscopic visibility would lack clinical utility, and more definitive histologic analysis was performed at 1 hour and later time points.

Fluorescein Angiography

Fluorescein angiography (FA) was performed immediately after placement of laser. As described previously,⁵⁰ 0.3 mL of fluorescein 10% (Fluorescite; Alcon Laboratories, Hünenberg, Switzerland) was slowly injected over 10 seconds into the marginal ear vein. Fundus photographs were taken with a Topcon TRC $\times 50$ fundus camera (Topcon, Itabashi, Japan) using a Kodak Megaplug Camera, Model 1.4, operated by the Winstation imaging software (Ophthalmic Imaging Systems, Inc, Sacramento, CA). Photographs were taken starting a few seconds after the injection and thereafter every 20 seconds for 5 minutes.

LIVE/DEAD Fluorescent Assay

The LIVE/DEAD Reduced Biohazard Viability/Cytotoxicity kit number 1 (Molecular Probes; Invitrogen, Carlsbad, CA) was used to assess RPE cell viability. This kit uses a SYTO green fluorescent

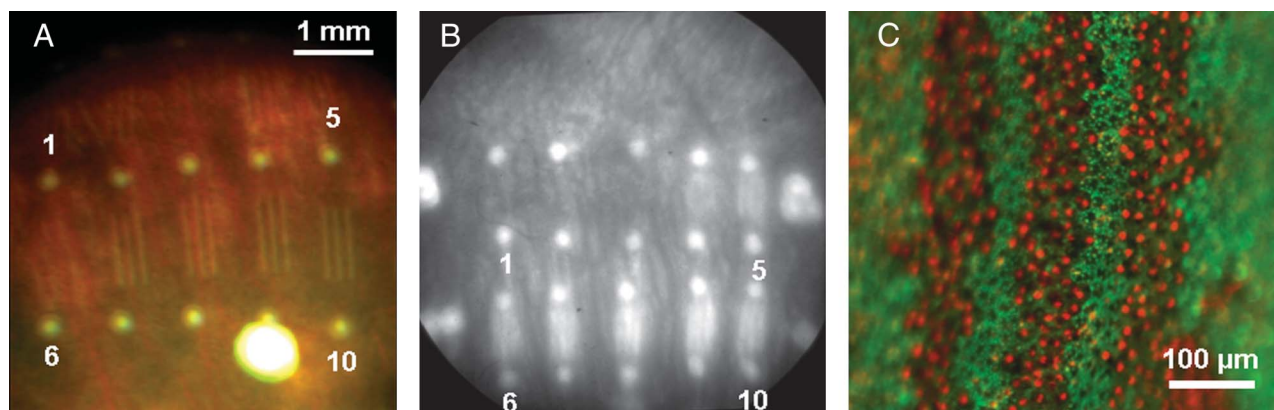


Fig. 1. Determination of ophthalmoscopic visibility, angiographic visibility, and live–dead staining thresholds of the retinal lesions. Sets of three lines are placed in a grid of increasing power (from top left to bottom right) with visible marker burns to facilitate localization. Sets of lines are referred to from 1 in the top left to 10 in the bottom right. **A.** Fundus photograph showing marker burns and patterns of 3 lines applied at increasing laser power. Ophthalmoscopic visibility threshold power is at the lesion 7. **B.** FA photograph showing marker spot lesions and 2 rows of line patterns of increasing laser power. The first three sets of lesions in the top row (1–3) are angiographically invisible; lesion 4 indicates angiographic threshold. **C.** Retinal pigment epithelium wholemount stained with LIVE/DEAD fluorescent assay, showing dead cells (red) within linear laser lesions.

nucleic acid stain to label all cells and a DEAD Red (ethidium homodimer-2) nucleic acid stain to label only cells with compromised cell membranes. The animals were killed 1 hour after laser application; the eyes were enucleated and the anterior portion (lens, cornea, and anterior chamber) was dissected away. The vitreous was then removed, and the irradiated portion of the retina, RPE, choroid, and sclera was sectioned. The retina was then gently peeled away from the RPE, and the fluorescent stain was placed directly on the RPE. These sections were incubated in a humid chamber for 20 minutes at room temperature, whereupon they were imaged on an inverted fluorescent microscope.

Statistical Analysis

The ED₅₀ is the median effective dose, or the laser power required to produce the specific effect in 50% of the measurements, with the specified effects including FA visibility, ophthalmoscopic visibility, and rupture of Bruch's membrane. The ED₅₀ measurements were made with a probit analysis using StatPlus (AnalytSoft, Vancouver, Canada) to calculate the thresholds in 4 to 8 eyes with 1 to 2 patterns per eye for each threshold measurement. The ED₅₀ values were

calculated to a minimum of 3 significant figures, and the ratios of the threshold values were thus also calculated to 3 significant figures.

Results

Thresholds Determination

The thresholds for rupture of Bruch's membrane, ophthalmoscopic and FA visibility, and live/dead assay were determined for beam sizes of 40 μm and 66 μm and dwell times of 15 microseconds and 60 microseconds. Figure 1 demonstrates the appearance of the line patterns using these techniques. Patterns included 10 groups of 3 lines in each, arranged in 2 rows, with conventional spot marker lesions in between. Laser power increases between these 10 groups from left to right and from top to bottom. In an example shown in Figure 1A, the bottom 4 lesions from the right (numbers 7–10) are visible ophthalmoscopically. With FA, the bottom 5 and the top 2 lesions on the right (numbers 4–10) are visible (Figure 1B). A higher magnification image of the 3-line pattern stained with live/dead assay is shown in Figure 1C.

Table 1. Threshold of Angiographic and Ophthalmoscopic Visibility and Rupture

Beam Size (μm)	Dwell Time (μs)	ED50 FA (mW)	ED50 Ophthal (mW)	ED50 Rupture (mW)	Ophthal/FA	Rupture/Ophthal	Rupture/FA
40	15	375 ± 146	1,043 ± 227	2,263 ± 206	3.10 ± 1.38	2.09 ± 0.13	7.16 ± 2.69
40	60	131 ± 43	216 ± 37	988 ± 48	1.81 ± 0.81	4.53 ± 0.23	7.05 ± 0.96
66	15	500 ± 122	1,253 ± 205	2,600 ± 200	2.58 ± 0.53	2.32 ± 0.22	5.08 ± 0.45
66	60	280 ± 67	458 ± 121	1,260 ± 65	1.65 ± 0.37	2.76 ± 0.15	4.46 ± 0.25

Mean and standard deviations of the ED₅₀ values for angiographic visibility, ophthalmoscopic visibility, and rupture for beam sizes of 40 μm and 66 μm and dwell times of 15 microseconds and 60 microseconds.

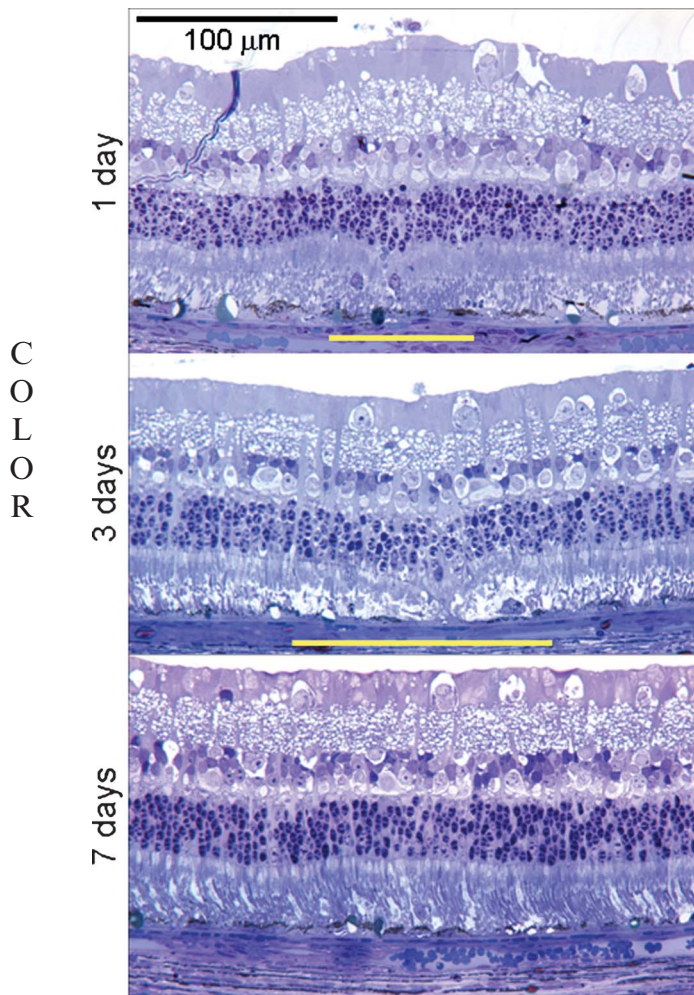


Fig. 2. Clinically invisible lesion at 1 day (A), 3 days (B), and 7 days (C) after treatment. Beam diameter $66\ \mu\text{m}$, dwell time 15 microseconds, and power 1,100 mW. All fundus photographs were taken with a $\times 20$ microscope objective. One day demonstrates RPE cell collapse and increased density of the outer segments. At 3 days, outer segments appear abnormal within a zone twice wider than the initial lesion, with edema between the outer segments and RPE. By 1 week, the RPE defect and the damage to the outer segments have largely resolved.

Measured thresholds of these visibility criteria and rupture are summarized in Table 1. The threshold of RPE damage is defined as ED_{50} level of the FA visibility. The ED_{50} for live/dead visibility corresponded exactly with that of FA ED_{50} (data not shown). The ED_{50} level of ophthalmoscopic visibility (OV) corresponds to the threshold of visible changes. Histologic analysis below demonstrated that this threshold corresponds to photoreceptor damage.

As expected, the ED_{50} for all thresholds increases with decreasing pulse duration. Because retinal rupture is an undesirable outcome, its threshold represents an upper limit of the safe dynamic range of the retinal treatment. The ratio of the threshold power for rupture to that of FA visibility defines the

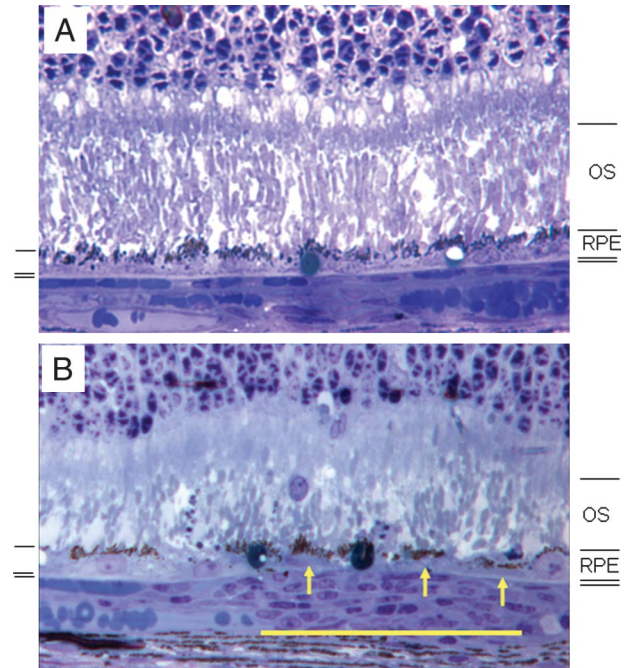


Fig. 3. Clinically invisible lesion at higher magnification ($\times 40$). **A.** Untreated retina demonstrating normal RPE-photoreceptor architecture. **B.** Retina at 1 day after laser treatment (clinically invisible, beam diameter $66\ \mu\text{m}$, 15 microseconds, and 1,100 mW). Retinal pigment epithelial cells collapse (yellow arrows) at the site of laser application (yellow line), and outer segments above them appear denser.

safe therapeutic window of this treatment. Smaller beam size ($40\ \mu\text{m}$ vs. $66\ \mu\text{m}$) resulted in a higher safety ratio: 7.16 versus 5.08 for 15-microsecond dwell time and 7.05 versus 4.46 for 60-microsecond dwell time ($P < 0.01$). Shorter exposures resulted in only a slight, statistically nonsignificant increase in the safe dynamic range: 7.05 versus 7.16 for a beam size of $40\ \mu\text{m}$ and 4.46 versus 5.08 for a beam size of $66\ \mu\text{m}$ for dwell times of 60 microseconds and 15 microseconds, respectively.

The treatment selectivity (i.e., RPE damage with sparing of photoreceptors) can be estimated as the ratio of the thresholds of OV to FA. In contrast to the safe therapeutic window, the dwell time markedly impacts lesion selectivity. Reducing the beam size from $66\ \mu\text{m}$ to $40\ \mu\text{m}$ resulted in minimal increase in the OV to FA ratio from 2.58 to 3.10 for 15-microsecond dwell time and from 1.65 to 1.81 for 60-microsecond dwell time. However, reducing dwell time from 60 microseconds to 15 microseconds resulted in a significant increase in the treatment selectivity, from 1.81 to 3.10 for $40\text{-}\mu\text{m}$ lesion size and from 1.65 to 2.58 for $66\text{-}\mu\text{m}$ lesion size ($P < 0.01$). Increasing the number of repetitions of the scan to 10 or 100 did not improve the safety window or the treatment selectivity (data not shown).

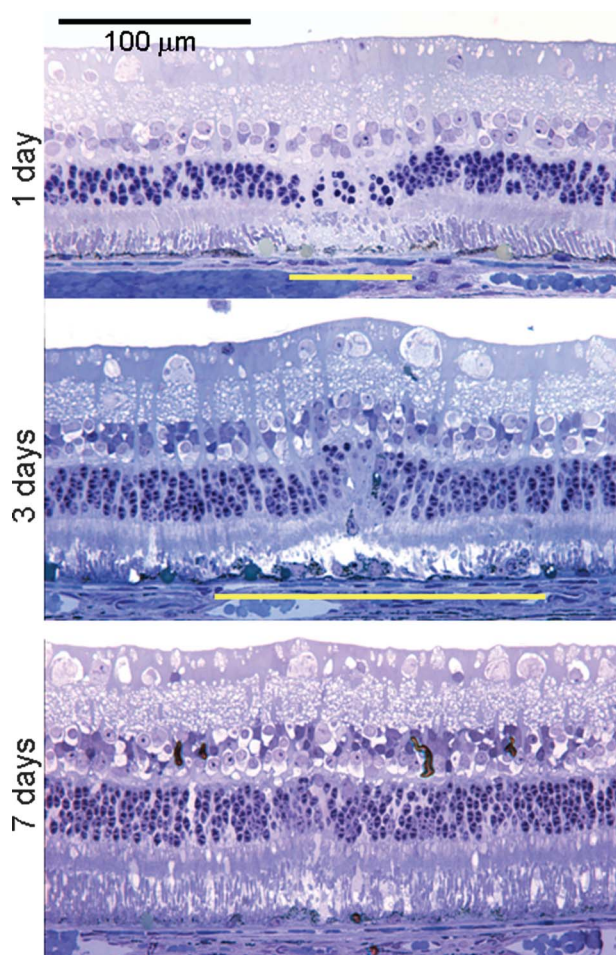


Fig. 4. Resolution of photoreceptor damage in the visible lesions. Dwell time 60 microseconds, laser power 1,000 mW, a single 66 μm line. Yellow bar indicates the extent of abnormal zone at the RPE–photoreceptor junction. Cellular loss is evident at 1 day in the ONL. The extent of nuclear dropout decreases at 3 days within the lesion; although the photoreceptor–RPE junction shows a widening of the area of disturbed, anatomy demonstrated loss of the vertical orientation of outer segments, edema between the inner and outer segments, and marked variability of the inner and outer segment thickness. At 7 days, a complete restoration of normal anatomy returns to both ONL and outer segments.

Healing of Retinal Line Lesions

Healing of retinal lesions produced by line scanning laser with microsecond exposures was followed over 2 months for both combinations of dwell times and beam sizes at 3 laser intensities. Representative lesions are shown in Figures 2–5.

In initially ophthalmoscopically invisible lesions at 1 day, RPE cells appear collapsed and outer segments appear more heavily stained with toluidine blue and increased in density (Figures 2 and 3). There is no evidence of loss of nuclei in the outer nuclear layer (ONL), although the photoreceptor outer segments do

demonstrate disorganization. At 3 days, both above the original lesion and also in the adjacent initially unaffected areas, the outer segments appear in an oblique orientation, edema exist between outer segments and RPE, and the outer segment thickness shows marked variability. At 3 days, there is no evidence of photoreceptor death and nuclear loss for ophthalmoscopically invisible lesions (Figure 2), whereas this is noted for visible lesions (Figure 4). The average width of these ophthalmoscopically invisible lesions at 3 days was 118 μm (SD, 9.5 μm), which is twice the width of the laser beam. Photoreceptors regain their normal morphology by 1 week (Figure 2).

Visible lesions were associated with photoreceptor death within 1 day of treatment (Figures 4 and 5). These lesions exhibited cellular loss at 1 day, with pyknosis and reduced numbers of nuclei in the ONL, hypopigmentation of the inner and outer segments, heavier staining with toluidine blue at round foci at the inner segment/outer segment junction, oblique orientation of the outer segments, and some edema between the RPE and photoreceptors. The inner retina was well preserved at all periods. In the single line lesion (Figure 4), damage in the ONL decreases at 3 days and resolves by 7 days. However, the abnormality at the photoreceptor–RPE junction widens significantly at 3 days compared with the initial lesion width and then resolves by 7 days.

Placement of 3 adjacent line lesions separated by 2 beam diameters altered the healing dynamics remarkably (Figure 5). At 1 day, these lesions exhibited findings typical of single line lesions described above, that is, pyknosis and reduced numbers of nuclei in the ONL, minor displacement of the ONL into the photoreceptor (PR) inner segments, slight edema and retinal thickening at the site of the laser patterns. However, at 3 days a dramatic change is noted in the surrounding photoreceptor regions: the vertical orientation of the outer segments is replaced with a haphazard arrangement, edema exists between inner and outer segments, and inner and outer segment thickness shows marked variability. At the laser sites, the lesions show minimal pyknosis and greatly reduced numbers of nuclei in the ONL, increased displacement of the ONL into the PR inner segments, edema, and retinal thickening. By 2 weeks, continuity of the ONL and photoreceptor anatomy were restored. Small patches of RPE hypertrophy persist at 2 months (Figure 5, arrows), but relatively normal anatomy of the outer segments was restored. In addition, density of the inner and outer segments layers and ONL appeared decreased both within the region of laser exposure and in the surrounding 120 μm .

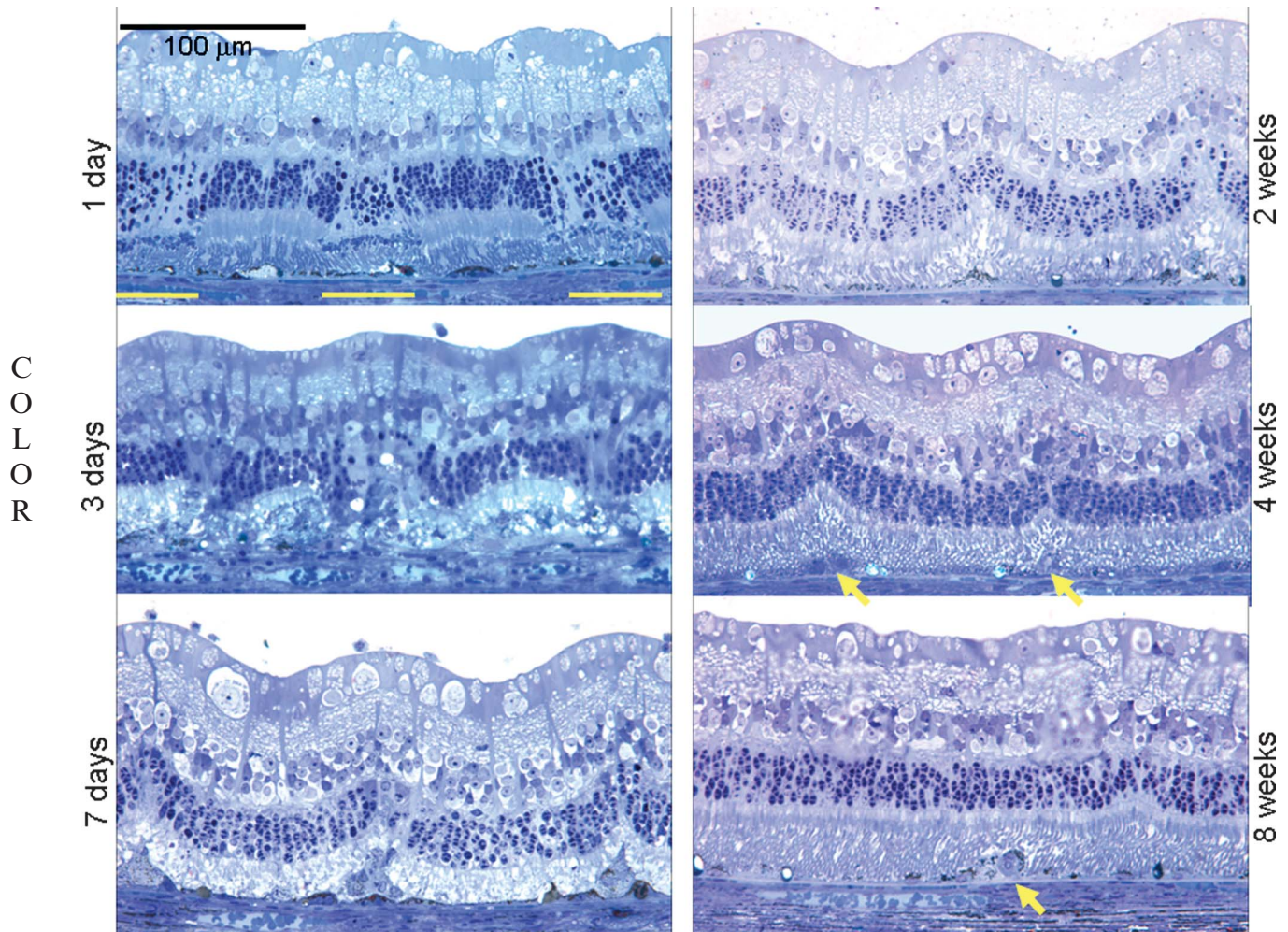


Fig. 5. Healing dynamics of a three-line pattern with line separations of two beam diameters. The laser parameters are identical to Figure 4. At 1 day, there is pyknosis and nuclear dropout in the ONL. At 3 days, a dramatic change in normal anatomy is noted in the surrounding photoreceptor regions. By 2 weeks, nuclear continuity and photoreceptor anatomy are largely restored. The retina flattens by 2 months, while some RPE hypertrophy persists (yellow arrow).

Discussion

Retinal pigment epithelium dysfunction occurs in several macular diseases, including age-related macular degeneration, diabetic macular edema, and CSC. This suggests a need for RPE-specific therapies, which SRT can achieve with microsecond pulses or the rapid scanning of a continuous laser.^{45,51}

We find that 15-microsecond and 60-microsecond retinal exposures produced by line scanning mode of the PASCAL laser damages the RPE without a loss of photoreceptors. Decreasing dwell time (increasing scanning speed) results in improved selectivity of the damage. As has been established previously,¹⁴ the safe therapeutic window is defined by the maximum intensity divided by the minimum intensity required for a desired outcome while avoiding an undesirable side effect. Because angiographic visibility corresponds to RPE damage, and retinal rupture should be avoided,

the therapeutic window for the treatment of RPE would be the ratio of the threshold power for rupture to that of FA visibility. Ophthalmoscopic visibility of the lesion corresponds to photoreceptor damage, and therefore therapeutic window of selective RPE treatment (aka, treatment that does not damage photoreceptors) is defined by the ratio of threshold powers for ophthalmoscopic and angiographic visibility. We find that a single line scanning approach (i.e., no repetitive scanning) provides a sufficiently large safety window of 4.5 to 7.2. For comparison, safe therapeutic window of conventional photocoagulation with 100-millisecond pulses is approximately 4.¹⁴

The dynamic range increased for decreasing exposure duration and also for decreasing lesion width. For our beam sizes (40 and 66 μm) and pulse durations (15 and 60 μs), reducing the beam diameter was the most efficient means to increase the therapeutic window. In contrast, selectivity of RPE

treatment, as determined by the ratio of OV to FA, was improved more by decreasing the dwell time.

Even if the threshold of ophthalmic visibility is exceeded, only relatively mild photoreceptor damage appears and it resolves without retinal scarring or gliosis within 1 week. Although lesions resulting from the dense patterns of three lines heal slower—perhaps because of more limited capacity of adjacent photoreceptors to migrate into lesions—by 2 months, photoreceptor continuity was restored in all cases, without scarring. These findings suggest that if the threshold of photoreceptor damage was inadvertently exceeded (e.g., because of pigmentation variation), permanent scars or scotomas would not ensue. This added safety is an attractive feature of microsecond laser for clinical use in the macula.

At 3 days after visible burn formation, mild abnormalities appear in the photoreceptor outer segments beyond the zone of RPE damage (Figure 4). This secondary effect of detaching and shortening of the outer segments from the underlying RPE may be because of proliferation and migration of surrounding RPE cells to restore continuity to the damaged area, which has been demonstrated to occur within one week.¹⁵ Redistribution of the photoreceptors by lateral migration from the unaffected areas into the damage zone restores continuity of the photoreceptor layer, with ONL cell density slightly reduced adjacent to the lesions, as we observed. This rearrangement and depletion of photoreceptors is even more evident in dense patterns of multiple lines, as shown in Figure 5.

In contrast to a previous study by Framme et al,⁴⁵ we do not find that multiple scans improve the safety or selectivity of the treatment. This difference could be because of the greater role of thermal diffusion and heat accumulation in our approach because it involves larger beam size (40 and 66 vs. 18 μm) and longer exposures (15 and 60 vs. 7.5 μs).

Selective treatment of RPE using a line scanning laser is a promising new modality characterized by enhanced selectivity and lack of permanent retinal structural sequelae. These features are particularly desirable when considering macular therapy. Moreover, a high beam velocity enables rapid treatment of relatively large retinal areas. For example, with a beam size of 60 μm , a 15-microsecond exposure time is achieved with a scanning velocity of 4 m/s. At such speed, 24 mm^2 can be treated within 100 milliseconds. For comparison, the total coagulated area using the modified Early Treatment Diabetic Retinopathy Study or mild macular grid photocoagulation does not exceed 6 mm^2 .⁵² The entire macula can be treated with a line scanning laser within a time shorter than a single conventional exposure.

Key words: microsecond pulse duration, retinal laser photocoagulation, retinal pigment epithelium, scanning laser, selective retinal therapy.

Acknowledgments

The authors thank Roopa Dalal for histological preparations; Resmi Charalel for lesion size measurements, stimulating discussion, and assistance with animal care and handling; and Phil Huie for assistance with animal care and handling.

References

1. Kapany NS, Peppers NA, Zweng HC, Flocks M. Retinal photocoagulation by lasers. *Nature* 1963;199:146–149.
2. Little HL, Zweng HC, Peabody RR. Argon laser slit-lamp retinal photocoagulation. *Trans Am Acad Ophthalmol Otolaryngol* 1970;74:85–97.
3. Jennings PE, MacEwen CJ, Fallon TJ, Scott N, Haining WM, Belch, JJ. Oxidative effects of laser photocoagulation. *Free Radic Biol Med* 1991;11:327–330.
4. Matsumoto M, Yoshimura N, Honda Y. Increased production of transforming growth factor-beta 2 from cultured human retinal pigment epithelial cells by photocoagulation. *Invest Ophthalmol Vis Sci* 1994;35:4245–4252.
5. Sanchez MC, Luna JD, Barcelona PF, et al. Effect of retinal laser photocoagulation on the activity of metalloproteinases and the alpha(2)-macroglobulin proteolytic state in the vitreous of eyes with proliferative diabetic retinopathy. *Exp Eye Res* 2007;85:644–650.
6. Spranger J, Hammes HP, Preissner KT, Schatz H, Pfeiffer AF. Release of the angiogenesis inhibitor angiostatin in patients with proliferative diabetic retinopathy: association with retinal photocoagulation. *Diabetologia* 2000;43:1404–1407.
7. Early Treatment Diabetic Retinopathy Study Research Group. Treatment techniques and clinical guidelines for photocoagulation of diabetic macular edema. Early Treatment Diabetic Retinopathy Study report number 2. *Ophthalmology* 1987;94:761–774.
8. Smiddy WE, Fine SL, Quigley HA, Hohman RM, Addicks EA. Comparison of krypton and argon laser photocoagulation. Results of stimulated clinical treatment of primate retina. *Arch Ophthalmol* 1984;102:1086–1092.
9. Smiddy WE, Patz A, Quigley HA, Dunkelberger GR. Histopathology of the effects of tuneable dye laser on monkey retina. *Ophthalmology* 1988;95:956–963.
10. Birngruber R, Hillenkamp F, Gabel VP. Theoretical investigations of laser thermal retinal injury. *Health Phys* 1985;48:781–796.
11. Marshall J, Mellerio J. Pathological development of retinal laser photocoagulations. *Exp Eye Res* 1967;6:303–308.
12. Sramek C, Paulus Y, Nomoto H, Huie P, Brown J, Palanker D. Dynamics of retinal photocoagulation and rupture. *J Biomed Opt* 2009;14:034007.
13. Higgins KE, Meyers SM, Jaffe MJ, Roy MS, de Monasterio FM. Temporary loss of foveal contrast sensitivity associated with panretinal photocoagulation. *Arch Ophthalmol* 1986;104:997–1003.
14. Jain A, Blumenkranz MS, Paulus Y, et al. Effect of pulse duration on size and character of the lesion in retinal photocoagulation. *Arch Ophthalmol* 2008;126:78–85.
15. Paulus YM, Jain A, Gariano RF, et al. Healing of retinal photocoagulation lesions. *Invest Ophthalmol Vis Sci* 2008;49:5540–5545.

16. Shimura M, Yasuda K, Nakazawa T, Tamai M. Visual dysfunction after panretinal photocoagulation in patients with severe diabetic retinopathy and good vision. *Am J Ophthalmol* 2005;140:8–15.
17. Early Treatment Diabetic Retinopathy Study Research Group. Focal photocoagulation treatment of diabetic macular edema. Relationship of treatment effect to fluorescein angiographic and other retinal characteristics at baseline: ETDRS report no. 19. *Arch Ophthalmol* 1995;113:1144–1155.
18. Morgan CM, Schatz H. Atrophic creep of the retinal pigment epithelium after focal macular photocoagulation. *Ophthalmology* 1989;96:96–103.
19. Schatz H, Madeira D, McDonald HR, Johnson RN. Progressive enlargement of laser scars following grid laser photocoagulation for diffuse diabetic macular edema. *Arch Ophthalmol* 1991;109:1549–1551.
20. Lewen RM. Subretinal neovascularization complicating laser photocoagulation of diabetic maculopathy. *Ophthalmic Surg* 1988;19:734–737.
21. Lewis H, Schachat AP, Haimann MH, et al. Choroidal neovascularization after laser photocoagulation for diabetic macular edema. *Ophthalmology* 1990;97:503–510.
22. Guyer DR, D'Amico DJ, Smith CW. Subretinal fibrosis after laser photocoagulation for diabetic macular edema. *Am J Ophthalmol* 1992;113:652–656.
23. Lovestam-Adrian M, Agardh E. Photocoagulation of diabetic macular oedema—complications and visual outcome. *Acta Ophthalmol Scand* 2000;78:667–671.
24. Rutledge BK, Wallow IH, Poulsen GL. Sub-pigment epithelial membranes after photocoagulation for diabetic macular edema. *Arch Ophthalmol* 1993;111:608–613.
25. Hudson C, Flanagan JG, Turner GS, Chen HC, Young LB, McLeod D. Influence of laser photocoagulation for clinically significant diabetic macular oedema (DMO) on short-wavelength and conventional automated perimetry. *Diabetologia* 1998;41:1283–1292.
26. Ishiko S, Ogasawara H, Yoshida A, Hanada K. The use of scanning laser ophthalmoscope microperimetry to detect visual impairment caused by macular photocoagulation. *Ophthalmic Surg Lasers* 1998;29:95–98.
27. Mainster MA. Decreasing retinal photocoagulation damage: principles and techniques. *Semin Ophthalmol* 1999;14:200–209.
28. Sinclair SH, Alaniz R, Presti P. Laser treatment of diabetic macular edema: comparison of ETDRS-level treatment with threshold-level treatment by using high-contrast discriminant central visual field testing. *Semin Ophthalmol* 1999;14:214–222.
29. Striph GG, Hart WM Jr, Olk RJ. Modified grid laser photocoagulation for diabetic macular edema. The effect on the central visual field. *Ophthalmology* 1988;95:1673–1679.
30. Busch EM, Gorgels TG, Van Norren D. Filling-in after focal loss of photoreceptors in rat retina. *Exp Eye Res* 1999;68:485–492.
31. Zwick H, Edsall P, Stuck BE, et al. Laser induced photoreceptor damage and recovery in the high numerical aperture eye of the garter snake. *Vision Res* 2008;48:486–493.
32. Blumenkranz MS, Yellachich D, Andersen DE, et al. Semi-automated patterned scanning laser for retinal photocoagulation. *Retina* 2006;26:370–376.
33. Al-Hussainy S, Dodson PM, Gibson JM. Pain response and follow-up of patients undergoing panretinal laser photocoagulation with reduced exposure times. *Eye* 2008;22:96–99.
34. Muqit MM, Marcellino GR, Gray JC, et al. Pain responses of Pascal 20 ms multi-spot and 100 ms single-spot panretinal photocoagulation: Manchester Pascal Study, MAPASS report 2. *Br J Ophthalmol* 2010; Jun 16 [Epub ahead of print].
35. Nagpal M, Marlecha S, Nagpal K. Comparison of laser photocoagulation for diabetic retinopathy using 532-nm standard laser versus multispot pattern scan laser. *Retina* 2010;30:452–458.
36. Roeder J, Michaud NA, Flotte TJ, Birngruber R. Response of the retinal pigment epithelium to selective photocoagulation. *Arch Ophthalmol* 1992;110:1786–1792.
37. Roeder J, Hillenkamp F, Flotte T, Birngruber R. Micro-photocoagulation: selective effects of repetitive short laser pulses. *Proc Natl Acad Sci U S A* 1993;90:8643–8647.
38. Roeder J, Brinkmann R, Wirbelauer C, Laqua H, Birngruber R. Subthreshold (retinal pigment epithelium) photocoagulation in macular diseases: a pilot study. *Br J Ophthalmol* 2000;84:40–47.
39. Framme C, Walter A, Prahs P, et al. Structural changes of the retina after conventional laser photocoagulation and selective retina treatment (SRT) in spectral domain OCT. *Curr Eye Res* 2009;34:568–579.
40. Lee H, Alt C, Pitsillides CM, Lin CP. Optical detection of intracellular cavitation during selective laser targeting of the retinal pigment epithelium: dependence of cell death mechanism on pulse duration. *J Biomed Opt* 2007;12:064034.
41. Elsner H, Porsken E, Klatt C, et al. Selective retina therapy in patients with central serous chorioretinopathy. *Graefes Arch Clin Exp Ophthalmol* 2006;244:1638–1645.
42. Elsner H, Klatt C, Liew SH, et al. [Selective retina therapy in patients with diabetic maculopathy]. *Ophthalmologie* 2006;103:856–860.
43. Brinkmann R, Roeder J, Birngruber R. Selective retina therapy (SRT): a review on methods, techniques, preclinical and first clinical results. *Bull Soc belge Ophtalmol* 2006;302:51–69.
44. Friberg TR, Karatza EC. The treatment of macular disease using a micropulsed and continuous wave 810-nm diode laser. *Ophthalmology* 1997;104:2030–2038.
45. Framme C, Schuele G, Roeder J, Kracht D, Birngruber R, Brinkmann R. Threshold determinations for selective retinal pigment epithelium damage with repetitive pulsed microsecond laser systems in rabbits. *Ophthalmic Surg Lasers* 2002;33:400–409.
46. Roeder J, Brinkmann R, Wirbelauer C, Laqua H, Birngruber R. Retinal sparing by selective retinal pigment epithelial photocoagulation. *Arch Ophthalmol* 1999;117:1028–1034.
47. Framme C, Alt C, Schnell S, Sherwood M, Brinkmann R, Lin CP. Selective targeting of the retinal pigment epithelium in rabbit eyes with a scanning laser beam. *Invest Ophthalmol Vis Sci* 2007;48:1782–1792.
48. Birngruber R. Choroidal circulation and heat convection at the fundus of the eye: implications for laser coagulation and the stabilization of retinal temperature. In: Wolbarsht ML, ed. *Laser Applications to Medicine and Biology*. Vol 5. New York, NY: Plenum Press; 1991: 277–362.
49. Turner KW. Hematoxylin toluidine blue-phloxinate staining of glycol methacrylate sections of retina and other tissues. *Stain Technol* 1980;55:229–233.
50. Maia M, Kellner L, de Juan E Jr, et al. Effects of indocyanine green injection on the retinal surface and into the subretinal space in rabbits. *Retina* 2004;24:80–91.
51. Framme C, Schuele G, Roeder J, Birngruber R, Brinkmann R. Influence of pulse duration and pulse number in selective RPE laser treatment. *Lasers Surg Med* 2004;34:206–215.
52. Committee for the Diabetic Retinopathy Clinical Research Network. Comparison of the modified Early Treatment Diabetic Retinopathy Study and mild macular grid laser photocoagulation strategies for diabetic macular edema. *Arch Ophthalmol* 2007;125:469–480.